

# applied optics

## Ultra-high-temperature resistant distributed Bragg reflector fiber laser based on type II-IR fiber Bragg gratings

XUANTUNG PHAM,<sup>1,2</sup> JINHAI SI,<sup>1,\*</sup> TAO CHEN,<sup>1</sup> ZHEN NIU,<sup>1</sup> AND XUN HOU<sup>1</sup>

<sup>1</sup>Key Laboratory for Physical Electronics and Devices of the Ministry of Education and Shaanxi Key Lab of Information Photonic Technique, School of Electronics and Information Engineering, Xi'an Jiaotong University, No. 28, Xianning West Road, Xi'an, 710049, China <sup>2</sup>Le Quy Don Technical University, Hanoi 122314, Vietnam

Received 5 February 2020; revised 2 March 2020; accepted 3 March 2020; posted 3 March 2020 (Doc. ID 389871); published 25 March 2020

We demonstrate a distributed Bragg reflector fiber laser that is capable of long-term operation at ultra-high temperatures. To form the laser cavity, a piece of Er-doped fiber is fusion spliced to a pair of type II-IR gratings, which are written using a femtosecond laser with a phase mask. Saturated gratings with different reflectivities are fabricated by varying the position of the grating region relative to the fiber core center. An eccentric grating with a relatively low reflectivity is chosen as the laser output coupler, while a regular grating with a higher reflectivity is used as the laser's high-reflection reflector. After an annealing process, the laser performance is tested at high temperatures. The results show that the laser can operate with a stable output wavelength and no output power degradation at high temperatures up to 1000°C. © 2020 Optical Society of America

https://doi.org/10.1364/AO.389871

#### 1. INTRODUCTION

Fiber lasers have attracted considerable interest in the field of optical fiber sensors. They not only possess the advantages of fiber grating sensors, such as inherent self-referencing and multiplexing capabilities, but also offer superior performance in terms of sensitivity, sensing resolution, and signal-to-noise ratio (SNR) [1–3]. In fiber laser sensing systems, distributed Bragg reflector (DBR) fiber lasers with attractive properties in simplicity and compactness have been widely used [4–7]. For any sensing applications in high-temperature environments, thermal resistance is a key issue. Nevertheless, a regular DBR fiber laser can hardly operate in high-temperature environments, resulting from the thermal degradation of its fiber Bragg grating (FBG) reflectors. Thus far, research efforts have been dedicated to improving the thermal resistance of DBR fiber lasers using FBG reflectors with high thermal resistance [8-13]. Lai et al. have realized a DBR fiber laser with a sustainable temperature of 600°C by directly fabricating the laser cavity in an Er/Yb-codoped fiber using a femtosecond laser and the point-by-point technique [9]. Ran et al. have presented an ultra-short DBR fiber laser using type IIa FBGs, which were fabricated by using a 193 nm ArF excimer laser and the overexposure method [10]. This laser can also withstand a high temperature of 600°C. Chen et al. have demonstrated a DBR fiber laser with high temperature resistance of 750°C by using a pair of regenerated

gratings and a long Er-doped fiber of 15 cm [11]. Grobnic *et al.* have directly fabricated type II-IR FBGs (II-IR FBGs) using an 800 nm femtosecond laser and a phase mask in a heavily Er/Yb-co-doped fiber to form a DBR fiber laser [12]. This laser can operate at temperatures up to 850°C. However, the output wavelength of this laser was unstable at high temperatures, as mode hopping was occasionally observed. Moreover, these DBR fiber lasers mentioned above can withstand temperatures that are still lower than those of reported FBGs, such as type II-IR FBG fabricated in standard Ge-doped telecom fiber (Corning SMF-28), which can be stable at temperatures of over 1000°C [14].

To form a DBR fiber laser with stable operation at different temperatures, the consistency of two FBG reflectors in their thermal responses is significant. Two FBG reflectors of DBR fiber lasers generally include a high-reflection FBG (HR-FBG)-based output coupler and a partial-reflection FBG (PR-FBG)-based laser output coupler (OC). The partial-reflection OC is generally obtained by tailoring the grating strength or grating length of the FBG. For the method of controlling the FBG grating strength, the OC commonly has a slightly weaker or even the same grating strength compared with the HR-FBG to ensure that the Bragg wavelength and thermal stability of these two gratings can be the same [10,11,15]. In this case, the reflectivities of the OC and HR-FBG are almost identical, resulting in a low laser threshold as well as low output

<sup>\*</sup>Corresponding author: jinhaisi@mail.xjtu.edu.cn

power. For the method of controlling the FBG grating length, both a 193 nm excimer laser with the beam scanning technique and a femtosecond laser with the point-by-point technique are powerful options [8,9,16]. Particularly the latter can flexibly fabricate FBGs with different grating lengths (reflectivities) that could survive at high temperatures up to 1000°C [17,18]. However, this method requires a high-accuracy and costly positioning system.

In this paper, we demonstrate a DBR fiber laser that can withstand an ultra-high temperature of 1000°C. The laser cavity consists of a piece of Er-doped fiber and a pair of II-IR FBG reflectors, which are fabricated using a femtosecond laser and a phase mask. By adjusting the position of the grating region relative to the fiber core center, saturated gratings with different reflectivities are fabricated. An eccentric grating with relatively low reflectivity and a regular grating with higher reflectivity are used as the laser OC and high-reflection reflector, respectively. The thermal response of the formed laser is investigated after an annealing process. The laser maintains stable operation at temperatures up to 1000°C with no performance degradation observed over a long testing time of 5 h. The results open a potential scheme to design and implement fiber laser sensors for ultra-high-temperature circumstances.

### 2. EXPERIMENTAL SETUP

The DBR laser consisted of two matched II-IR FBGs, including a HR-FBG-based and a PR-FBG-based laser OC, which were fusion spliced to both ends of an Er-doped fiber as shown in Fig. 1. The Er-doped fiber is commercially available (Liekki Er 80-8/125, manufactured by nLinght Inc., Finland) and has a core diameter of 8  $\mu m$  and a cladding diameter of 125  $\mu m$ . Its peak absorption at 976 nm was measured to be 25 dB/m. A 976 nm laser diode was used as a pump source, and it is coupled into the laser cavity through a 980/1550 nm wavelength division multiplexer (WDM).

The II-IR FBG fabricated in rare-earth-doped fibers has shown a high insertion loss of 1.5 to 2 dB [12,19], which is much higher than that of the II-IR FBG fabricated in commercial passive fibers (around 0.6 dB) and is unfavorable for laser oscillation [20]. Thus, the II-IR FBG reflectors of the DBR laser were inscribed in SMF-28 fiber (core diameter ~8 μm) instead of the Er-doped fiber using a femtosecond laser and a phase mask. The fabrication system of these gratings is shown in Fig. 2(a). An amplified Ti:sapphire laser system (Libra-USP-HE, Coherent Inc., USA) generating 120 fs pulses at a center wavelength of 800 nm and a repetition rate of 1 kHz was adopted. The 10 mm diameter Gaussian beam with 750 μJ pulse energy was focused using a cylindrical lens (focal length of 25 mm) through a second-order phase mask

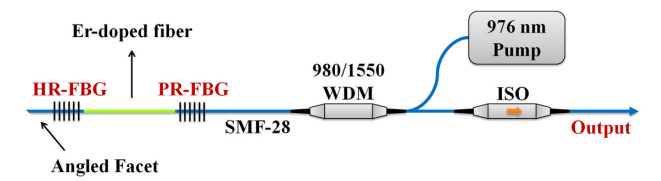


**Fig. 1.** Schematic diagram of the DBR fiber laser. WDM, wavelength division multiplexer; ISO, isolator.

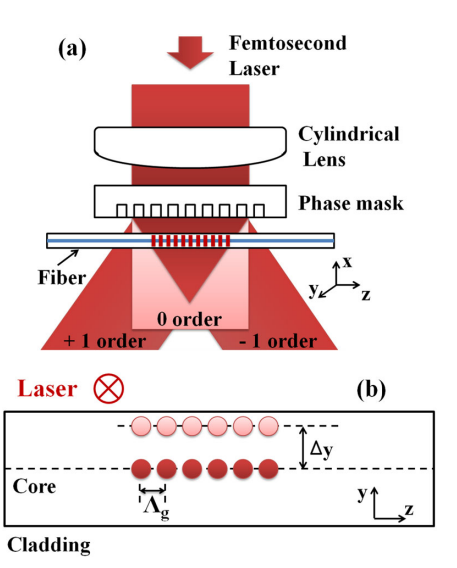


**Fig. 2.** Schematic diagrams of the (a) fabrication system of type II-IR FBGs and (b) grating distribution of fabricated gratings in the fiber core.

(pitch of 2.142 µm) into the fiber. The fiber was clamped on a piezoelectric platform, which can achieve a three-dimensional translation with a maximum length of 20  $\mu$ m. In the fabrication process, the focused laser beam center was precisely aligned with the fiber core center based on the diffractive pattern of the laser beam going through the fiber. The distance between the fiber and the phase mask was about 300 µm, where diffractive beams from the phase mask would generate multiple-beam interference [21]. The multiple-beam interference field has higher peak intensity than that of the two-beam interference field that is commonly used for the fabrication of II-IR FBGs [14,22]. The second-order phase mask was used here instead of a first-order one (pitch of 1.071 µm) because compared with the first-order mask, the high-order mask enables multiple-beam interference to occur at a farther distance from the mask (along with the laser incident direction) [20]. Thus, the distance between the high-order mask and the fiber can be farther than that in the case when the first-order mask is used, thereby avoiding the damage of the mask resulting from the high-peak laser intensity in II-IR FBG fabrication. Different from the fabrication method of type II-IR gratings in Refs. [12,14], here the fiber was fixed instead of scanning during the FBG fabrication process. The II-IR FBGs were fabricated by laser exposure at intervals, which can suppress the thermal effects and increase the formation efficiency of FBGs [3]. The exposure and interval times were set to 0.1 s and 5 s using a mechanical beam shutter. With the fabrication condition in our experiments, the white light generation that is coincident with type II-IR grating formation was observed. A broadband source with a wavelength range of 1520–1580 nm and an optical spectrum analyzer (Yokogawa, AQ6370D) with a spectral resolution of 0.02 nm were used to monitor and record the grating transmission spectrum during the fabrication process. According to free-space Gaussian beam optics, after the laser Gaussian beam is focused using the cylindrical lens, the focal line width is  $W = 2\omega \approx 2\lambda f/\pi \omega_0 \approx 2.5 \mu m$ , where  $\lambda$  is the laser wavelength, f is the focal length of the cylindrical lens, and  $\omega_0$  is the incident beam radius. As the focal line width

of the focused laser beam is much smaller than the fiber core diameter ( $\sim$ 8 µm), the grating region of fabricated II-IR FBGs only covered a portion of the fiber core in the y direction as shown in Fig. 2(b). By precisely adjusting the relative position between the focused laser beam and fiber core center using the piezoelectric platform, eccentric II-IR FBGs can also be fabricated with different displacements in the y direction ( $\Delta y$ ) of the grating region.

#### 3. RESULTS AND DISCUSSION

To fabricate II-IR FBG reflectors with different reflectivities, we investigated the influence of the grating region position in the y direction relative to the fiber core center on the grating reflectivity. First, we fabricated a regular II-IR FBG whose grating region is precisely at the fiber core center. The total exposure time to obtain a regular grating with a saturated spectrum was about 0.8 s, which is the same as in our previous report [3]. Then we fabricated several eccentric II-IR FBGs with different displacements in the y direction  $(\Delta y)$  of the grating region from 1 to 3.5 µm. These eccentric gratings were also fabricated with the total exposure time of 0.8 s, and saturated spectra were obtained accordingly. The grating lengths of these gratings were all the same and measured to be 3.5 mm. Their grating periods were approximately 2.14 µm, equal to the phase mask period. These fabricated gratings possess typical spectra of type II-IR FBGs with strong cladding modes as shown in Fig. 3 [14].

It can be observed that the Bragg resonances of these II-IR FBGs are all well matched. The regular II-IR FBG possesses the highest resonance intensity of over 45 dB at its Bragg wavelength. When the displacement of the grating region increases, the resonance intensity of the grating at its Bragg wavelength decreases, which is similar to the case of highly localized FBGs [23]. The resonance intensity of the eccentric grating at its Bragg wavelength is approximately 29, 18.5, 10.6, and 6.8 dB for displacements of 1, 2, 3, and 3.5 μm, respectively. Meanwhile, the 3 dB bandwidth of the grating also decreases from 1.55 to 0.74 nm as the displacement of the grating region increases from 0 to 3.5 μm. Moreover, the out-of-band insertion loss of these gratings is from 0.5 to 0.8 dB, which is much smaller than that of type II-IR FBGs fabricated in Er/Yb-co-doped fiber (insertion loss of 1.5—2 dB) [19]. These results suggest that

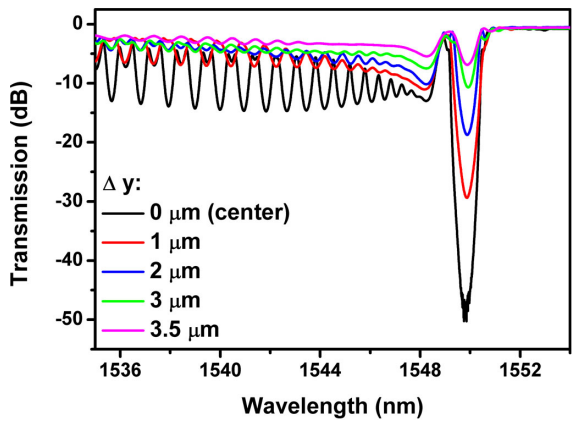


**Fig. 3.** Transmission spectra of II-IR FBGs with different displacements in the y direction ( $\Delta y$ ) of the grating region from 0 to 3.5  $\mu$ m relative to the fiber core center.

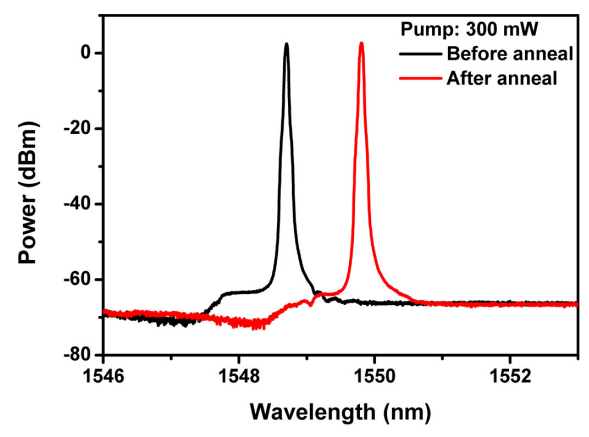


**Fig. 4.** Laser spectra at room temperature of 28°C before and after the annealing process. A pump power of 300 mW is used.

saturated II-IR FBGs with well-matched Bragg resonances and different reflectivities can be fabricated by adjusting the grating region position in the fiber core. As a result, two II-IR FBGs with desired reflectivities can be chosen to use as laser reflectors. Since these II-IR FBGs were fabricated in the same conditions, they are supposed to have the same thermal resistance, ensuring laser stability at high temperatures.

From the fabricated II-IR FBGs mentioned above, which possess well-matched Bragg resonances, we selected the regular grating with the highest reflectivity and the 3 µm eccentric grating with relatively lower reflectivity to use as the high-reflection reflector and laser OC, respectively. Considering the higher insertion loss of II-IR FBGs in comparison with that of type I-IR FBGs, a 9 cm long Er-doped fiber was used to provide sufficient gain for the laser oscillation [13]. Its two ends were fusion spliced to the selected reflectors to form the laser cavity. The entire length of the laser cavity was around 10 cm, and the longitudinal mode space was estimated to be approximately 8 pm [5]. Besides, the 3 dB bandwidth of the laser OC was around 0.8 nm, which was much larger than the longitudinal mode space. Consequently, multiple longitudinal modes can satisfy the conditions for laser oscillation [5]. The threshold power of the formed laser was approximately 20 mW. The laser output spectrum at the pump power of 300 mW is shown in Fig. 4. Subsequently, the formed laser was put into a tube oven and annealed at 1000°C for 5 h to decay the unstable grating structures of its reflectors before its thermal response and stability were tested. This tube oven can provide good control of the temperature with an accuracy of  $\pm 1^{\circ}$ C at temperatures from 300°C to 1200°C. After the annealing process, the laser output spectrum was remeasured and is shown in Fig. 4. The laser threshold increases from 20 to 25 mW and the output wavelength shifts from 1549.81 to 1548.70 nm, resulting from the thermal degradation of the laser reflectors. The 3 dB bandwidth of the laser also decreases from approximately 0.05 to 0.04 nm, which is much larger than the longitudinal mode space. This result indicates that the laser operates in multiple longitudinal modes.

The performance of the DBR fiber laser was tested at temperatures from 300°C to 1000°C. At each temperature, the test duration was set to 30 min to stabilize the temperature in

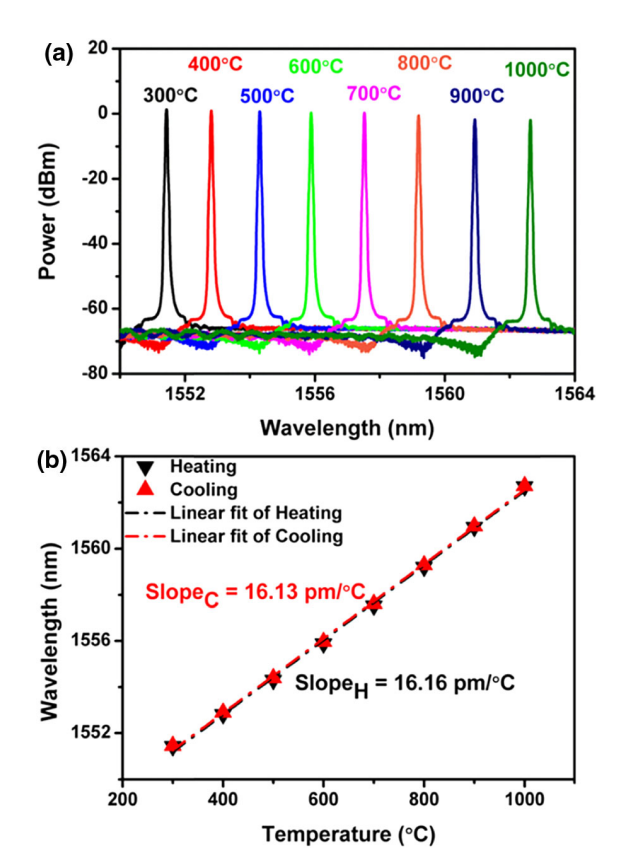


**Fig. 5.** (a) Laser output spectra at different temperatures. (b) Laser output wavelength versus temperature in the heating and cooling processes.

the tube oven and obtain a stable spectrum. The laser spectra at different temperatures are shown in Fig. 5(a). The SNR of the laser output is better than 60 dB in the tested temperature range. Figure 5(b) shows the laser output wavelength in response to temperature variations in the heating and cooling processes. The good linear relationships (regression coefficients of over 99.8%) between the laser output wavelength and temperature are obtained in both heating and cooling processes with almost identical sensitivities of 16.16 pm/°C and 16.13 pm/°C, respectively. Two linear fitting lines almost overlap as shown in Fig. 5(b), indicating the high repeatability of laser output wavelength at different temperatures. A quadratic relationship between the laser output wavelength and temperature can be achieved in the range from room temperature to 1000°C, similar to the case reported in Ref. [3]. This is because the temperature sensitivity of FBG reflectors in the low-temperature region is commonly smaller than that in high-temperature region [3,11]. Here the average temperature sensitivity is approximately 10.15 pm/°C at temperatures from room temperature to 300°C (obtained from the data in Figs. 4 and 5).

The laser stability was further tested at  $1000^{\circ}$ C for 5 h, and the results are shown in Fig. 6. The laser output wavelength is highly stable at an average wavelength of 1562.702 nm with a standard deviation of 0.011 nm. The laser output remains at an average power of -1.69 dBm without obvious degradation over the whole duration of 5 h. These results indicate that the formed laser exhibits significant resistance at high temperatures

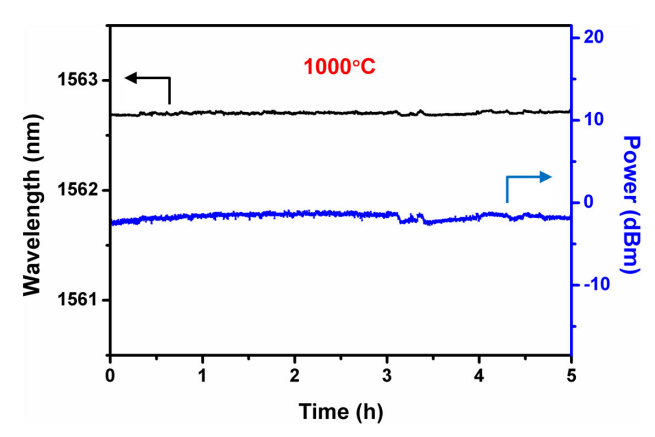


**Fig. 6.** Long-term stability of laser output at 1000°C over 5 h.

up to 1000°C, which is better than that of reported DBR fiber lasers [11,12].

### 4. CONCLUSIONS

In summary, we present a DBR fiber laser that can survive at ultra-high temperatures. Type II-IR FBGs are used as laser reflectors, and they are fabricated with a femtosecond laser and a phase mask. Saturated gratings with different reflectivities are fabricated by adjusting the grating region position in the fiber core. An eccentric grating with relatively low reflectivity and a regular grating with higher reflectivity are used as the laser OC and high-reflection reflector. After an annealing process, the formed DBR laser is capable of long-term operation with stable output properties at high temperatures up to 1000°C. The laser possesses a SNR of over 60 dB.

**Funding.** National Key Research and Development Program of China (2017YFB1104600); Key Research and Development Program of Shaanxi Province (2017ZDXM-GY-120); Fundamental Research Funds for the Central Universities (XJJ2016016).

**Disclosures.** The authors declare no conflicts of interest.

#### **REFERENCES**

- O. Hadeler, E. Rønnekleiv, M. Ibsen, and R. I. Laming, "Polarimetric distributed feedback fiber laser sensor for simultaneous strain and temperature measurements," Appl. Opt. 38, 1953–1958 (1999).
- W. Xie, Y. Zhang, P. Wang, and J. Wang, "Optical fiber sensors based on fiber ring laser demodulation technology," Sensors 18, 505 (2018).
- F. Huang, T. Chen, J. Si, X. Pham, and X. Hou, "Fiber laser based on a fiber Bragg grating and its application in high-temperature sensing," Opt. Commun. 452, 233–237 (2019).
- L. Shao, X. Dong, A. P. Zhang, H. Tam, and S. He, "High-resolution strain and temperature sensor based on distributed Bragg reflector fiber laser," IEEE Photon. Technol. Lett. 19, 1598–1600 (2007).
- Y. Zhang, B. O. Guan, and H. Y. Tam, "Ultra-short distributed Bragg reflector fiber laser for sensing applications," Opt. Express 17, 10050–10055 (2009).
- A. C. L. Wong, W. H. Chung, C. Lu, and H. Tam, "Composite structure distributed Bragg reflector fiber laser for simultaneous two-parameter sensing," IEEE Photon. Technol. Lett. 22, 1464–1466 (2010).

- B. Guan and S. Wang, "Fiber grating laser current sensor based on magnetic force," IEEE Photon. Technol. Lett. 22, 230–232 (2010).
- 8. B. O. Guan, Y. Zhang, H. J. Wang, D. Chen, and H. Y. Tam, "High-temperature-resistant distributed Bragg reflector fiber laser written in Er/Yb co-doped fiber," Opt. Express 16, 2958–2964 (2008).
- Y. Lai, A. Martinez, I. Khrushchev, and I. Bennion, "Distributed Bragg reflector fiber laser fabricated by femtosecond laser inscription," Opt. Lett. 31, 1672–1674 (2006).
- Y. Ran, F. R. Feng, Y. Z. Liang, L. Jin, and B. O. Guan, "Type IIa Bragg grating based ultra-short DBR fiber laser with high temperature resistance," Opt. Lett. 40, 5706–5709 (2015).
- R. Chen, A. Yan, M. Li, T. Chen, Q. Wang, J. Canning, K. Cook, and K. P. Chen, "Regenerated distributed Bragg reflector fiber lasers for high-temperature operation," Opt. Lett. 38, 2490–2492 (2013).
- D. Grobnic, S. J. Mihailov, and R. B. Walker, "Narrowband high temperature sensor based on type II laser cavity made with ultrafast radiation," in *Advanced Photonics* (Optical Society of America, 2014), paper BW2D. 5.
- X. Pham, J. Si, T. Chen, Z. Niu, F. Huang, and X. Hou, "Ultra-short DBR fiber laser with high-temperature resistance using tilted fiber Bragg grating output coupler," Opt. Express 27, 38532–38540 (2019).
- C. Smelser, S. J. Mihailov, and D. Grobnic, "Formation of type I-IR and type II-IR gratings with an ultrafast IR laser and a phase mask," Opt. Express 13, 5377–5386 (2005).
- F. R. Feng, Y. Ran, Y. Z. Liang, S. Gao, Y. H. Feng, L. Jin, and B. O. Guan, "Thermally triggered fiber lasers based on secondary-type-In Bragg gratings," Opt. Lett. 41, 2470–2473 (2016).

- Y. Lai, K. Zhou, K. Sugden, and I. Bennion, "Point-by-point inscription of first-order fiber Bragg grating for C-band applications," Opt. Express 15, 18318–18325 (2007).
- S. J. Mihailov, "Fiber Bragg grating sensors for harsh environments," Sensors 12, 1898–1918 (2012).
- H. Chikh-Bled, K. Chah, Á. González-Vila, B. Lasri, and C. Caucheteur, "Behavior of femtosecond laser-induced eccentric fiber Bragg gratings at very high temperatures," Opt. Lett. 41, 4048–4051 (2016).
- D. Grobnic, S. J. Mihailov, R. B. Walker, and C. W. Smelser, "Laser cavity made with ultrafast IR type II gratings in heavily doped Er-Yb fiber," in *Advanced Photonics Congress* (Optical Society of America, 2012), paper BW3E. 2.
- S. J. Mihailov, C. W. Smelser, D. Grobnic, R. B. Walker, P. Lu, H. Ding, and J. Unruh, "Bragg gratings written in all-SiO2 and Ge-doped core fibers with 800-nm femtosecond radiation and a phase mask," J. Lightwave Technol. 22, 94–100 (2004).
- C. W. Smelser, D. Grobnic, and S. J. Mihailov, "Generation of pure two-beam interference grating structures in an optical fiber with a femtosecond infrared source and a phase mask," Opt. Lett. 29, 1730–1732 (2004).
- 22. D. Grobnic, C. Hnatovsky, and S. J. Mihailov, "Low loss type II regenerative Bragg gratings made with ultrafast radiation," Opt. Express 24, 28704–28712 (2016).
- J. Thomas, N. Jovanovic, R. G. Becker, G. D. Marshall, M. J. Withford, A. Tunnermann, S. Nolte, and M. J. Steel, "Cladding mode coupling in highly localized fiber Bragg gratings: modal properties and transmission spectra," Opt. Express 19, 325–341 (2011).